Journal of Climate Change Research 2024, Vol. 15, No. 4, pp. 415~426
DOI: https://doi.org/10.15531/KSCCR.2024.15.4.415

The cooling effect of vertical greening systems using solar radiation measurement

Zhao, Mengjia[*] · Kim, Eun Sub[*] and Lee, Dong Kun[**,***†]

[*]*PhD Student, Interdisciplinary Program in Landscape Architecture, Seoul National University, Seoul, Republic of Korea*
[**]*Professor, Department of Landscape Architecture and Rural System Engineering, College of Agriculture and Life Sciences, Seoul National University, Seoul, Republic of Korea*
[***]*Professor, Research Institute of Agriculture and Life Sciences, College of Agriculture and Life Sciences, Seoul National University, Seoul, Republic of Korea*

ABSTRACT

Vertical greening systems (VGS) can effectively mitigate the urban heat island effect in urban canyons with dense high-rise buildings. This study evaluates the cooling effect of VGS on solar radiation and atmospheric temperature. A thermodynamic analysis was utilized to assess the impact of VGS on outdoor thermal comfort. CNR4 equipment collected data on long-wave and short-wave radiation from *Fatsia japonica* plants. These data formed the basis for simulation analyses with the Envi-met model, which showed that VGS exhibit significant diurnal surface temperature variations in the urban environment during the summer months. Areas with VGS had higher temperatures than those of high albedo walls (HAW) from 2:00 to 4:00 and recorded lower temperatures than those of HAW between 13:00 and 15:00. VGS absorb short-wave and long-wave radiation better than HAW. The average short-wave radiation of VGS is 43.91 W/h^2, compared to 31.50 W/h^2 for HAW, while the average long-wave radiation of VGS is 2.82 W/h^2, compared to -1.53 W/h^2 for HAW. Envi-met simulations indicate that the surface temperature of the VGS decreases after 15:00, to about 0.1°C cooler than HAW. The data from July 15 indicate that VGS significantly outperformed HAW in terms of cooling the maximum temperature at 13:00 and stabilizing the minimum temperature at 3:00. Furthermore, the extent of the cooling effect of the VGS was approximately 1.5 meters. This demonstrates that VGS, as an eco-friendly solution, can improve the urban thermal environment, increase the urban greening rate, and promote ecologically balanced development.

Key words: Urban Heat Island, Green Infrastructure, CFD, Energy Balance, Evapotranspiration Effect

1. Introduction

The main cause of the urban heat island effect is the increased absorption of solar radiation by the urban surface relative to the surrounding environment (Alsaad et al., 2022). This phenomenon is caused by two factors; high-density urban buildings expand the vertical surface area of the city, and an increase in the number of buildings leads to an increase in urban density and insulation (Kim et al., 2023). Although cities currently cover less than 2% of the earth's surface, they produce more than 60% of global greenhouse gas emissions and contribute to rising temperatures (The Paper, 2021). With 2.5 billion more people expected to live in urban areas by 2050, greenhouse gas emissions will continue to increase and temperatures will continue to rise if nothing changes.

The city itself is like a giant heat absorber and accumulator (Oliveira and Salles, 2020). The urban heat island effect caused by human activities and public space design will become more significant (Shahmohamadi et

†**Corresponding author :** dklee7@snu.ac.kr (08826, Department of Landscape Architecture and Rural System Engineering, College of Agriculture and Life Sciences, Seoul National University, 1 Gwanak-ro, Gwanak-gu, Seoul, Republic of Korea. Tel. +82-2-880-4875)

ORCID Zhao, Mengjia 0009-0008-5287-8620 Lee, Dong Kun 0000-0001-7678-2203
Kim, Eun Sub 0000-0003-2206-5203

Received: December 22, 2023 / Revised: April 3, 2024 1st, May 13, 2024 2nd, June 3, 2024 3rd / Accepted: July 25, 2024

al., 2011). However, the city's current design is insufficient to effectively withstand rising temperatures. With the rapid development of modern industrialized cities, the number of buildings has increased and the amount of land available for greening has decreased (Paudyal et al., 2019). Problems such as air pollution, water pollution, ecological imbalance and heat island effect have seriously affected the quality of life of urban residents and threatened the healthy development of modern cities (Peng et al., 2021).

Vertical greening is an effective measure to mitigate the urban heat island effect (Price et al., 2015). The application of vegetation cover on building exteriors serves to decrease ambient temperatures and reduce energy consumption (Hayes et al., 2022; Saiz et al., 2006), thereby optimizing the utilization of constrained urban spaces and enhancing green coverage.

VGS lower ambient temperatures, improve urban microclimates and reduce the impact of the heat island effect on cities through transpiration, water absorption and wind regulation (Hayes et al., 2022). The ability of vegetation to absorb and reflect solar radiation, especially at midday on sunny days, reduces heat build-up on street and building surfaces, further improving the urban microclimate (Medl et al., 2017). Studies have shown that the valley temperature of urban streets with vertical greening is 0.83°C lower than that of cities without vertical greening, and that large-scale application of vertical greening technology can significantly reduce the cooling load of urban buildings by 5% to 8% and lower urban air temperature by about 0.7 to 0.9°C, which reduces the heat island effect by almost half. In addition, the application of vertical greening technology can effectively reduce summer building energy consumption by 9% to 59%, reducing the amount of heat emitted to the city by air conditioners (Bevilacqua, 2021).

Short-wave radiation from the sun and long-wave radiation emitted by the earth are important factors affecting the thermal processes in plant canopies (Erell et al., 2014), prompting extensive research in this area by many scholars (Alexandri and Jones, 2008; Shafiee et al.,2020; Tan et al.,2014; Zhao et al., 2022). Shafiee, Elham et al investigated the effect of plant walls on ambient air. The results of the study showed that the presence of plant strong reduces the ambient air temperature (Shafiee et al., 2020). The results showed that roof gardens were able to intercept about 90% or more of solar radiation. Additionally, vertical green cover (VCF) was found to absorb and reduce the amount of solar radiation by up to 86% (Chen et al., 2019).

Envi-met contributes to the simulation and mitigation of the urban heat island effect (Cortes et al., 2022). Despite its widespread used to simulate various scenarios in urban environments, it is crucial to strive for a proper understanding and rational use of the software's parameters (Crank et al., 2018). This is because the software is based on Computational Fluid Dynamics (CFD), and software accuracy in CFD has always been a challenge, with different models, accuracies, and meteorological parameters leading to different results (Shafiee et al., 2020; Yang et al., 2019).

In recent years, addressing the urban heat island effect has become a focal point of research, with the Envi-met software emerging as a prevalent tool for simulations and predictions (Cortes et al., 2022). Without sufficient validation, the use of unreliable parameters can lead to severe theoretical mistakes. In this study, we conducted experimental validation of the thermodynamic aspects of VGS to evaluate outdoor thermal comfort. The greening involved planting *Fatsia japonica*, and we used a CNR4 measuring device to record short-wave and long-wave radiation, as well as albedo. The Envi-met model was then utilized to validate these measurements and to assess the microclimate effects of vertical greening. The experiments and simulations will provide insights into the role of vertical greening systems in microclimate regulation and offer a reliable scientific basis for improving the urban thermal environment and enhancing outdoor comfort.

2. Material and methods

2.1. The experimental setup

This study was conducted on the roof of Academic Building 38 (coordinates 37.2717, 126.5701) at Seoul

Fig. 1. North-facing green facade building at Seoul National University Development Corporation

National University, Korea. The experiment was divided into two groups, VGS and HAW, to evaluate the performance of VGS in terms of outdoor cooling and thermal insulation. The system in the VGS group consisted of plants and soil, while the other group was a control group with only soil and no plants (Djedjig et al., 2015). This was done to exclude the effect of soil thickness on plant cooling to ensure that the cooling and insulating effects of the VGS were evaluated. In order to compare it with a normal wall, the study also measured parameters such as long-wave radiation, short-wave radiation and temperature of a normal white wall in the same area (Zhang et al., 2019) The VGS has dimensions of 1800 mm×1200 mm and consists of plant modules with dimensions of 300 mm×150 mm arranged in an array of 12×4. These modules are located in front of the wall at a distance of 40 cm (Koch et al., 2020) Each group of VGS consist of two sets of portable green walls, which are designed to place the experiments in the same environment in order to exclude errors caused by factors such as environment and time of day. To minimize the effect of shadows on the experiment, the VGS were oriented towards the north (Fig. 1).

The vertical drip irrigation technology in this experimental VGS uses wick irrigation technology (Cameron et al., 2014). The principle is that the left and right planting

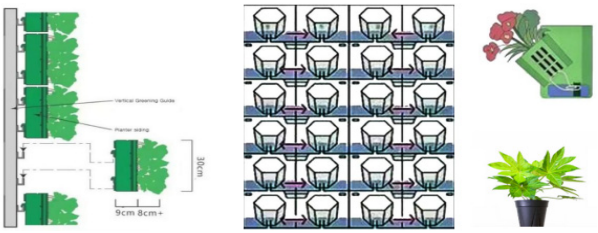

Fig. 2. Vertical Green System design with irrigation system

tanks can pass water to each other, the outer basin of each layer of planting tanks can store water, the inner basin stores water up to the height of the drainage column, and the water will flow to the next layer, the water storage space is sealed, and the water does not contact with the wall, so it will not leak or wet the wall. The water in the storage layer is transported to the soil through a cotton rope, the storage system does not touch the soil and keeps the water clear (Fig. 2).

The plant for vertical greening is *Fatsia japonica*, the reason for choosing this plant is that *Fatsia japonica* has a large leaf area and is easy to propagate, making it suitable as a potted plant. Another reason is that *Fatsia japonica* is a tropical plant that is sensitive to light and can adapt to stronger sunlight, making it an ideal plant to withstand strong solar radiation (Carroll and Spengler, 2021). *Fatsia japonica* is a local native plant that is better adapted to local climatic conditions and is also easy to care for, making it a potential plant for mitigating the heat island in the corresponding city. Therefore, plants with diameters of 25 ~ 40 cm were selected as wall greening plants for this experiment.

2.2. Data collection and equipment

In this experiment, a separate CR1000 data logger (Campbell Scientific, USA) was used to collect data on longwave radiation, shortwave radiation, etc. for comparing the differences in absorption and reflection of long and shortwave radiation among the three experimental groups. To ensure the accuracy of the data, the CNR4 sensor has a measurement height of 1.2 m and a measurement distance of 1 m thermal camera

Table 1. Equipment list and details of each measurement sensor (Kim et al., 2023)

Variable	Sensor type	Manufacturer	Unit	Accuracy
Air temperature	S-thb-m002	Hobo, US	°C	±0.21°C
Relative Humidity	S-thb-m002		%	±2.5%
Wind speed	S-wcf-m003		m/s	±1.1 m/s
Thermal camera	COX CG640	Smart Measurement, Republic of Korea	°C	±2°C
Solar radiation	CNR4	Campbell Scientific, US	W/ [-]	<4%

(COX-CG640, Smart Measurement, Korea) with an accuracy of ±2°C and a resolution of 640 by 480 pixels was used from a horizontal position of 2.5 m from the surface in order to measure the surface temperature. To avoid surprises during the experiment, a thermal camera with 24 h video recording was used for automatic real-time data collection. The collected data was converted into image form and surface temperature data was extracted at 1 min intervals. In addition, air temperature and relative humidity (measured using the Onset Hobo S-THB-M002 with an accuracy of ±0.21°C and ±2.5%) and wind speed (measured using the Onset Hobo s-wcf-m003 with an accuracy of ±1.1 m/s) were recorded (Kim et al., 2023). Table 1 (Kim et al., 2023) summarizes information on these data logging devices and associated parameters.

The measurement period was from July 15 to July 17, 2022 (3 days). During this period, the meteorological data in the Seoul area showed an average temperature of 26.6°C, with a maximum temperature during the heat wave of 30°C. The relative humidity averaged 78% and the wind speed was 5.57 m/s. The data were measured at one-minute intervals while maintaining a constant position during the data collection period.

2.3. Measurement solar radiation of VGS for Envi-met simulation

VGS utilize plant coverage on building exteriors, where photosynthesis and transpiration play a role in environment interactions (Su et al., 2024). These processes contribute to the reduction of heat absorption at the building surface, thereby decreasing the temperature of both the structure and its vicinity (Wong et al., 2010). Furthermore, during photosynthesis, plants absorb solar radiation energy and release water vapor into the air through transpiration. The evaporation of this water requires heat absorption, which additionally helps to lower the ambient temperature (Morakinyo et al., 2019). Collectively, these mechanisms enable VGS to mitigate the urban heat island effect and improve the local microclimate.

The law of conservation of energy allows us to analyze the relationship between vertical greening systems in terms of shortwave radiation energy income and energy output. Such a comparison helps to infer how much shortwave energy is absorbed by the VGS in a given time period, i.e., the relationship between the input shortwave radiation and the output thermal radiation. VGS convert shortwave radiation energy through two processes: the absorption of energy from the sun's shortwave radiation by the plants and the release of heat by the plants as they release water. According to the law of conservation of energy, there is an energy balance relationship between these processes. By comparing the energy changes, it is possible to reveal the degree of absorption of solar radiation by the vertical greening system (Lauster et al., 2014). Because of the full coverage of plant canopy area in this experiment, it is desirable not to consider the canopy coverage.

$$\text{Absorbed Shortwave Radiation} = \text{Incoming SR} - \text{Outgoing SR} \quad (1)$$

Plants and vegetative coverings in vertical greening systems can influence the absorption and release of

long-wave radiation from building surfaces (Zhao et al., 2022). Plants can reduce longwave radiation at night, which helps to reduce the amount of heat emitted from building surfaces, thus lowering the temperature of the surrounding environment. Plants release water into the surroundings through transpiration, resulting in heat absorption required for water evaporation. This process also helps to reduce the temperature of the surroundings (Zhang et al., 2022). The relationship between longwave radiation and vertical greening systems may be more pronounced at night or under low radiation conditions. Although the effect of longwave radiation on vertical greening systems may not be as significant as that of shortwave radiation, longwave radiation is still involved to some extent in the regulation and influence of vertical greening systems on the temperature of the surrounding environment.

Absorbed longwave Radiation
= Incoming LR − Outgoing LR (2)

2.4. Envi-met simulation

Envi-met is a three-dimensional numerical model for simulating urban microclimate, which simulates parameters such as temperature, humidity, wind speed and radiation in the atmospheric boundary layer (Ng et al., 2012). The model uses measurement data from 38 rooftops on the Seoul National University campus and records data such as air temperature, global radiation temperature, relative humidity, and wind speed at the same locations on three different dates. Based on these data, Envi-met created a geometric model of the campus rooftops, considering the effects of three-dimensional greening and zoning.

However, the software has some shortcomings that prevent it from accurately modeling an ordinary earth wall without greening. Therefore, the researchers set the greening value of the earth wall without greening to a minimum value. The greened and ungreened areas (VGS and HAW) were compared by adjusting the greening setting to the minimum value (about 1 cm) and the VGS setting to 30 cm for the greened portion (Fig. 3 ~ Fig. 5). Next, a simulation was conducted using the weather data of the day, with the main objective of verifying the cooling effect of these three different scenarios.

The scholarly assessment of surface temperature projections for VGS and HAW enables researchers to discern the influence of micro-scale urban features, including buildings, roadways, and vegetation, on the spatial distribution of air temperatures (Ali-Toudert et al., 2007). Such a thermodynamic investigation elucidates the role of urban greening initiatives in microclimate modification and furnishes empirical insights instrumental for urban environmental enhancement.

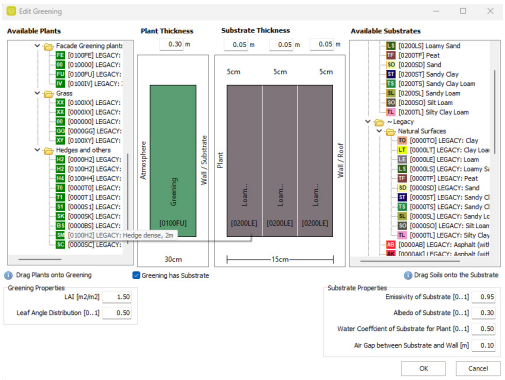

Fig. 3. Vertical green system for Envi-met simulation

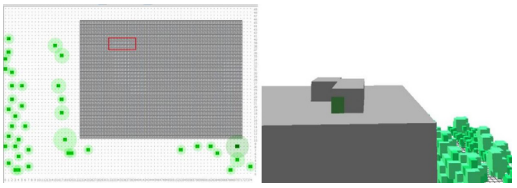

Fig. 4. Envi-met simulated building plans and renderings

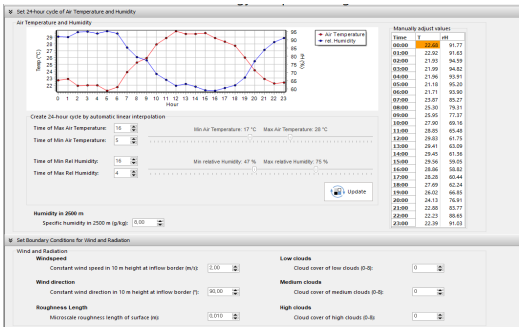

Fig. 5. Envi-met parameter table July 15

3. Results and discussion

3.1. VGS and HAW Surface temperature

In this experiment, the surface temperatures of both the vegetated VGS and HAW were quantified based on the collected data. The analysis of the overall trends indicates that the surface temperature fluctuations of both the VGS and HAW correspond with changes in ambient air temperature. However, the variation in surface temperature of HAW more closely aligns with that of the ambient temperature, whereas the range of temperature changes observed in VGS is more pronounced. For instance, observations from July 15 indicate that surface temperatures for both VGS and HAW commenced their ascent from 6:00. By 9:00 temperatures at the surfaces of both systems stabilized at 30°C. Subsequently, VGS temperatures remained above those of HAW until 14:00, at which point both systems recorded equal temperatures of 35°C. Thereafter, temperatures on the vegetated surfaces of VGS fell below those of HAW (Fig. 6).

HAWs are constructed using materials characterized by high reflectivity, which enhances their capability to reflect solar radiation and thereby minimize thermal gain (Nasir and Hassan, 2020). This reflective quality enables the surface temperature of HAWs to closely align with fluctuations in ambient air temperatures. In contrast, VGS typically includes multiple layers of soil, moisture, and vegetation, which have higher thermal mass and insulation. This allows VGS to absorb and retain heat for longer periods, resulting in a wider range of temperature fluctuations (Pan and Chu, 2016).

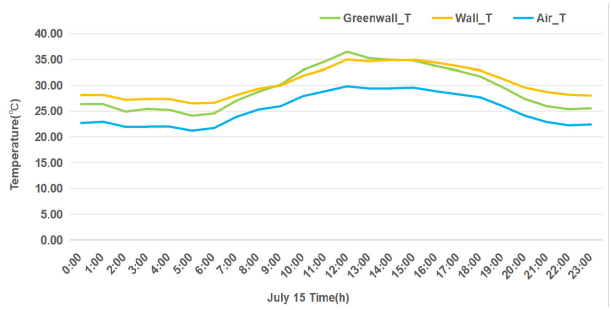

Fig. 6. Surface temperature for one day

3.2. Comparison of shortwave radiation output of three groups of experiments

This experiment uses empirical data to perform a comparative analysis of short-wave radiation absorption by VGS, non-vegetated surfaces, and HAW. Although the three surface types show analogous diurnal trends, distinct disparities in short-wave radiation absorption were evident (Fig. 7). Examination through the principles of energy conservation and data analysis yielded the following insights: The short-wave radiation absorption of the

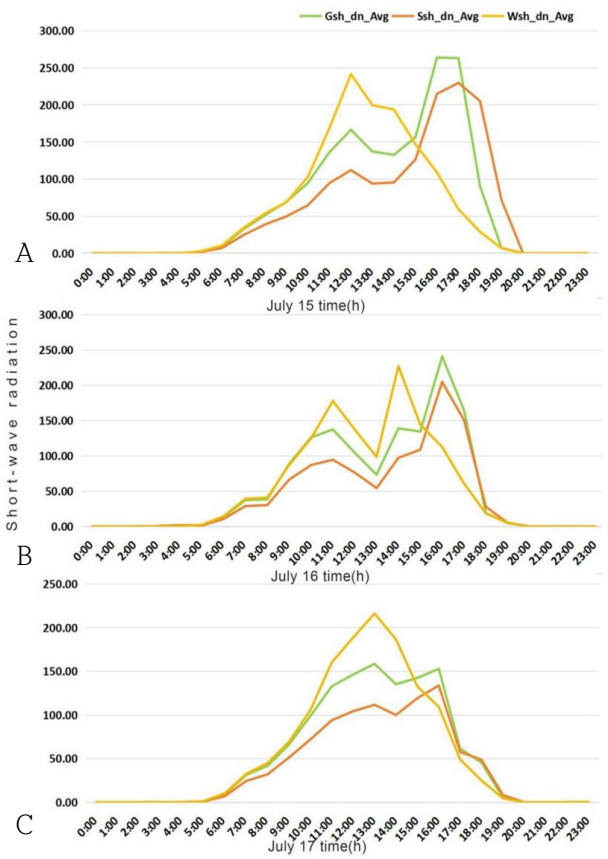

Fig. 7. A, B, C three groups of experimental shortwave radiation (Gsh_dn_Avg represents the average output of shortwave radiation from a vertical greening system with plants, Ssh_dn_Avg represents the average output of shortwave radiation from a vertical greening system without plants, and Wsh_dn_Avg represents the output of shortwave radiation from a High Albedo wall).

assessed surfaces exhibits substantial temporal variation. During the daytime, radiation absorption increases corresponding with peak solar radiation, whereas nocturnal intervals are characterized by a minimization of absorption due to the absence of solar input. Comparative assessments reveal that vegetated VGS (represented by the green line) and non-vegetated surfaces (denoted by the orange line) exhibit more pronounced short-wave radiation absorption than HAW (indicated by the yellow line). The mean absorption values are 54.47 W/m^2 for non-vegetated surfaces, 43.91 W/m^2 for VGS, and 31.50 W/m^2 for HAW. This difference is likely attributable to the greater thermal mass and diminished reflectivity of non-vegetated substrates (Pianella et al., 2017). Notably, absorption peaks coincide with solar zenith, typically occurring around noon. The peak value of HAW is much lower than that of the other evaluated surfaces, reflecting its higher reflectivity and reduced tendency to absorb short-wave radiation (Marino et al., 2017).

3.3. Comparison of longwave radiation output of three groups of experiments

In the experiment shown in Fig. 8, we compared the absorption of long-wave radiation by a VGS, a surface without vertical greening, and a HAW. The absorption of long-wave radiation increases with the rise in solar radiation after sunrise, and decreases as the intensity of solar radiation weakens, exhibiting diurnal variation characteristics consistent with the solar radiation cycle. Specifically, the VGS surface has the highest long-wave radiation absorption capacity, with an average absorption of 2.82 W/m^2, followed by the non-vegetated surface with 2.72 W/m^2, while the HAW surface has the weakest absorption capacity with -1.53 W/m^2. This difference in absorption capacity may be due to the HAW's highly reflective material, which reflects more long-wave radiation. In addition, the vegetation layer of VGS releases water through transpiration, and absorbs heat when water evaporates, which naturally reduces the absorption of long-wave radiation. This process manifests as a higher radiation absorption peak and a rapid temperature drop (Brar et al., 2015). Simultaneously, the shading effect of plants reduces direct solar radiation, affecting the process of heat absorption and release (Yang et al., 2021). Therefore, plant coverage is a key factor in regulating the absorption of long-wave radiation on the VGS surface and affecting the microclimate, providing an additional temperature regulation mechanism compared with surfaces without vegetation (Zhao et al., 2022).

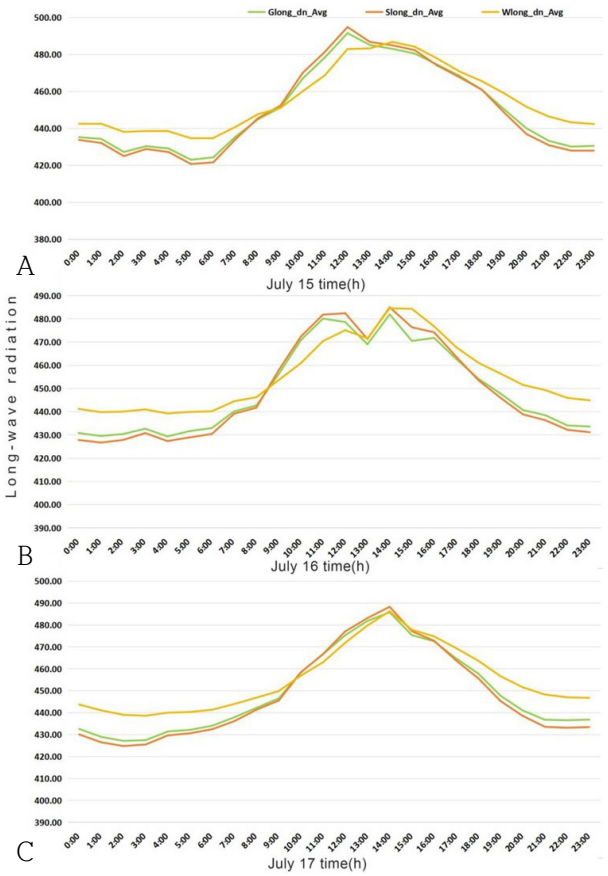

Fig. 8. A, B, C three groups of experimental longwave radiation (Gsh_dn_Avg represents the average output of longwave radiation from a vertical greening system with plants, Ssh_dn_Avg represents the average output of longwave radiation from a vertical greening system without plants, and Wsh_dn_Avg represents the output of longwave radiation from a High Albedo wall).

3.4. Envi-met potential air temperature

This simulation uses the measured data from July 15 to 17 for Envi-met simulation, and the results are consistent with the experimental data. The simulation results are shown in Analysis Table 2, where the value “green” indicates that the surface temperature of VGS is higher than HAW, the value “gray” indicates that the surface temperatures of the two systems are equal, and the value “orange” indicates that the surface temperature of VGS is lower than HAW. The overall trend shows that the surface temperature of VGS is higher than HAW in most time periods, especially from July 15 to 17, when VGS continued to show a higher temperature from 4:00 to 12:00. This phenomenon may be related to the presence of plants in VGS, and the cooling effect of plants through transpiration and shading is more obvious during the day. However, at night or during periods of weak solar radiation (i.e., 1:00, 2:00, and 14:00 to 24:00), the temperature of VGS is lower than or equal to the temperature of HAW, reflecting the slower heat release characteristics of VGS. In addition, the temperatures of VGS and HAW were equal at 2:00 on July 16 and between 13:00 and 14:00 on July 17, which may indicate that the two systems have similar thermal response dynamics under certain conditions. During the night and

Table 2. Comparison of temperature results for ENVI-met VGS and HAWs

Comparison of hourly temperature results for three days for VGS and HAWs						
	VGS>HAW VGS=HAW VGS<HAW		Unit: °C			
Day	July-15		July-16		July-17	
Time	15 VGS	15 HAW	16 VGS	16 HAW	17 VGS	17 HAW
01:00	27.31	27.33	26.60	26.61	26.92	26.94
02:00	26.97	26.98	26.61	26.61	26.43	26.43
03:00	26.04	26.04	25.01	24.99	25.52	25.48
04:00	25.05	25.02	24.40	24.38	24.85	24.82
05:00	24.21	24.14	25.04	23.99	24.44	24.40
06:00	23.73	23.66	23.58	23.55	24.37	24.32
07:00	23.78	23.69	23.62	23.58	24.40	24.44
08:00	24.09	23.96	23.78	23.69	24.86	24.66
09:00	24.36	24.21	23.91	23.73	24.96	24.76
10:00	24.66	24.47	24.03	23.89	25.07	24.79
11:00	25.02	24.87	24.35	24.11	24.38	24.12
12:00	25.18	25.01	24.77	24.60	25.58	25.48
13:00	25.36	25.36	24.83	24.51	25.81	25.81
14:00	26.49	26.56	25.25	25.25	26.26	26.26
15:00	26.18	26.26	25.71	25.79	27.11	27.20
16:00	26.56	26.64	25.95	26.03	27.72	27.33
17:00	27.06	27.11	26.12	26.24	27.73	27.79
18:00	27.55	27.58	26.20	26.21	28.18	28.21
19:00	27.82	27.85	26.60	26.64	28.22	28.28
20:00	27.72	27.79	26.95	26.99	28.44	28.50
21:00	27.50	27.52	27.43	27.48	28.27	28.30
22:00	27.99	28.06	27.77	27.82	27.70	27.72
23:00	28.35	28.38	27.52	27.55	27.55	27.57
24:00	27.90	27.92	27.22	27.28	27.58	27.63

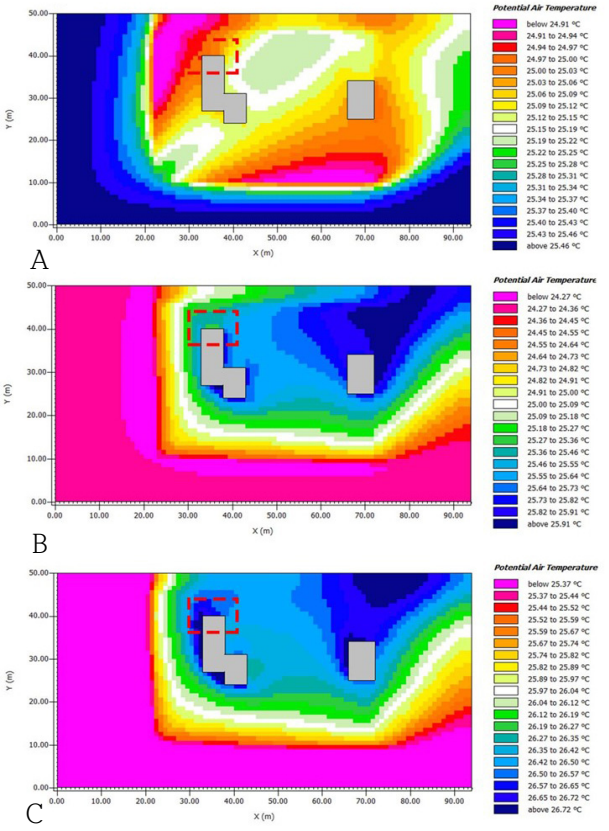

Fig. 9. A, B and C show the potential air temperatures at 04:00, 13:00, and 14:00 on July 15, respectively

from 15:00 to 24:00 when solar radiation is low, the VGS surface temperature is always lower than the HAW surface temperature, further emphasizing the potential effectiveness of VGS in cooling.

On July 15, changes in the surface temperatures of VGS and HAW were observed. At 4:00, the HAW surface temperature was approximately 0.06°C lower than the VGS, with the range of 24.97 ~ 25.00°C for HAW and 25.00 ~ 25.03°C for VGS (Fig. 9a). By around 13:00, the temperatures at the HAW and VGS surfaces were essentially equal (Fig. 9b). However, at about 14:00, the temperature of the HAW surface began to gradually increase and eventually exceeded that of the VGS surface, with temperature intervals of 26.50 ~ 26.57°C for HAW and 26.57 ~ 26.65°C for VGS (Fig. 9c). As a result, the temperature difference between the two gradually increases.

The potential air temperatures on July 16 and 17 showed similar trends to those on July 15, with HAW temperatures higher than VGS temperatures in the morning, and by 13:00-14:00 the same temperatures of both systems were the same, followed by HAW temperatures higher than VGS at 15:00.

3.5. Envi-met Comparison of maximum and minimum temperatures for one day

By comparing the potential air temperatures of the maximum and minimum air temperatures within the same day, the effect of greening on the distribution of air temperatures and the shading effect of the building can be analyzed. By observing the results on July 15, it was shown that the presence or absence of vertical greening on the buildings may have a cooling effect, but the effect was not significant (Fig. 10), only the extent of cooling changed, with the area of influence of VGS being larger than the area of influence of HAW, with an area distance of about 1.5 maters.

While earlier studies have made significant contributions to understanding the impact of VGS on urban heat island effects, they often focused on specific aspects like short-wave or long-wave radiation absorption

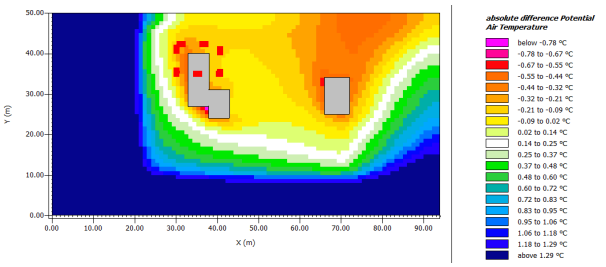

Fig. 10. Comparison of maximum and minimum temperatures for July 15 (3:00 and 15:00)

(Lee and Jim, 2019; Zhao et al., 2022). In contrast, this research takes a more holistic approach by integrating both short-wave and long-wave radiation analyses. This comprehensive perspective offers a deeper and more nuanced understanding of VGS performance across different times of the day.

Furthermore, prior research, though valuable, often did not fully account for the detailed thermodynamic properties and diurnal variations (Zhang et al., 2019). Specifically, during the early morning hours (2:00 to 4:00), VGS tend to have higher temperatures compared to HAW because the vegetation retains heat accumulated during the day. This heat retention results from the thermal mass of the vegetation and soil, which release heat more slowly than the reflective surfaces of HAW. In contrast, from 13:00 to 15:00, VGS exhibit lower temperatures than HAW due to their ability to absorb and dissipate solar radiation more efficiently. The plants in VGS provide shading and undergo transpiration, a process where water is evaporated from plant leaves, absorbing heat and cooling the surrounding air. This dual mechanism of shading and transpiration significantly enhances the cooling effect of VGS during the hottest part of the day, making them more effective than HAW in reducing surface and ambient temperatures.

ENVI-met has been widely used to simulate and mitigate the urban heat island effect (Cortes et al., 2022). Despite its widespread use, it is crucial to strive for a proper understanding and rational use of the software's parameters (Crank et al., 2018). One of the main limitations of previous ENVI-met studies is the challenge in achieving accurate CFD model outputs due to varying

model accuracies and meteorological parameters (Shafiee et al., 2020; Yang et al., 2019).

This research advances the existing knowledge by conducting experimental validation of the thermodynamic aspects of VGS, which ensures that the ENVI-met simulations are grounded in empirical data. By incorporating detailed measurements of long-wave and short-wave radiation, as well as temperature variations, our study provides a more reliable assessment of VGS's cooling effects and their impact on outdoor thermal comfort. This approach addresses the gaps in previous studies, which often relied on theoretical simulations without sufficient experimental validation.

The extent of the cooling effect of VGS is also noteworthy. ENVI-met simulations indicate that the surface temperature of VGS decreases after 15:00, being about 0.1°C cooler than HAW. The data from July 15 indicate that VGS significantly outperformed HAW in terms of cooling the maximum temperature at 13:00 and stabilizing the minimum temperature at 3:00. Furthermore, the cooling effect of VGS extends to approximately 1.5 meters, which is a clear advantage over HAW.

This research not only underscores the effectiveness of VGS in urban heat island mitigation but also highlights their potential for improving urban thermal environments and enhancing outdoor comfort. The findings support the continued research and development of VGS as an eco-friendly solution for urban cooling.

4. Conclusion

This investigation employs both empirical measurements and Envi-met simulations to ascertain the outdoor cooling efficacy of VGS. The findings indicate that the diurnal temperature trajectories of VGS and HAW display congruent patterns, yet manifest divergent specific temperatures. During the morning and afternoon intervals, the surface temperatures of HAW consistently surpass those of VGS; conversely, at midday, temperatures of VGS occasionally exceed those recorded for HAW. Regarding radiative absorption, VGS demonstrates superior capability in both long-wave and short-wave radiation absorption compared to HAW. While simulation outcomes corroborate the observed temperature trends, there is a notable discrepancy between the simulated surface temperatures and the actual measurements. The results affirm the potential of VGS in mitigating surface temperatures, particularly through enhanced absorption of both short-wave and long-wave radiation, thereby outperforming HAW. These outcomes provide robust empirical support for continued research into, and refinement of, VGS design and applications.

Acknowledgments

This work was supported by Korea Environment Industry & Technology Institute (KEITI) through 'Climate Change R&D Project for New Climate Regime.', funded by Korea Ministry of Environment (MOE) (2022003570004).

References

Alexandri E, Jones P. 2008. Temperature decreases in an urban canyon due to green walls and green roofs in diverse climates. Build Environ 43(4): 480-493. doi: 10.1016/j.buildenv.2006.10.055

Ali-Toudert F, Mayer H. 2007. Effects of asymmetry, galleries, overhanging façades and vegetation on thermal comfort in urban street canyons. Sol energy 81(6): 742-754. doi: 10.1016/j.solener.2006.10.007

Alsaad H, Hartmann M, Hilbel R, Voelker C. 2022. The potential of facade greening in mitigating the effects of heatwaves in Central European cities. Build Environ 216: 109021. doi: 10.1016/j.buildenv.2022.109021

Bevilacqua P. 2021. The effectiveness of green roofs in reducing building energy consumptions across different climates. A summary of literature results. Renew Sustain Energy Rev 151: 111523. doi: 10.1016/j.rser.2021.111523

Brar VW, Sherrott MC, Jang MS, Kim S, Kim L, Choi M, Sweatlock LA, Atwater HA. 2015. Electronic modulation of infrared radiation in graphene plasmonic resonators. Nat Commun 6: 7032. doi: 10.1038/

ncomms8032

Cameron RW, Taylor JE, Emmett MR. 2014. What's 'cool' in the world of green façades? How plant choice influences the cooling properties of green walls. Build Environ 73: 198-207. doi: 10.1016/j.buildenv.2013.12.005

Carroll J, Spengler T. 2021. Japanese Aralia care: How to grow Fatsia Japonica. https://www.gardeningknowhow.com/houseplants/aralia-plants/japanese-aralia-care.htm.

Chen Q, Ding Q, Liu X. 2019. Establishment and validation of a solar radiation model for a living wall system. Energy Build 195: 105-115. doi: 10.1016/j.enbuild.2019.05.005

Cortes A, Rejuso AJ, Santos JA, Blanco A. 2022. Evaluating mitigation strategies for urban heat island in Mandaue city using ENVI-met. J Urban Manag 11(1): 97-106. doi: 10.1016/j.jum.2022.01.002

Crank PJ, Sailor DJ, Ban-Weiss G, Taleghani M. 2018. Evaluating the ENVI-met microscale model for suitability in analysis of targeted urban heat mitigation strategies. Urban Clim 26: 188-197. doi: 10.1016/j.uclim.2018.09.002

Djedjig R, Bozonnet E, Belarbi R. 2015. Experimental study of the urban microclimate mitigation potential of green roofs and green walls in street Canyons. Int J Low-Carbon Technol 10(1): 34-44. doi: 10.1093/ijlct/ctt019

Erell E, Pearlmutter D, Boneh D, Kutiel PB. 2014. Effect of high-albedo materials on pedestrian heat stress in urban street canyons. Urban Clim 10: 367-386. doi: 10.1016/j.uclim.2013.10.005

Hayes AT, Jandaghian Z, Lacasse MA, Gaur A, Lu H, Laouadi A, Ge H, Wang L. 2022. Nature-Based Solutions (NBSs) to mitigate Urban Heat Island (UHI) effects in Canadian cities. Buildings 12(7): 925. doi: 10.3390/buildings12070925

Kim ES, Yun SH, Lee DK, Kim NY, Piao ZG, Kim SH, Park S. 2023. Quantifying outdoor cooling effects of vertical greening system on mean radiant temperature. Dev Built Environ 15: 100211. doi: 10.1016/j.dibe.2023.100211

Koch K, Ysebaert T, Denys S, Samson R. 2020. Urban heat stress mitigation potential of green walls: A review. Urban For Urban Green 55: 126843. doi: 10.1016/j.ufug.2020.126843

Lauster M, Remmen P, Fuchs M, Teichmann J, Streblow R, Müller D. 2014. Modelling long-wave radiation heat exchange for thermal network building simulations at urban scale using Modelica. Proceedings of the 10th International Modelica Conference; 2014 Mar 10~Mar 12; Lund University. Lund, Sweden: Modelica Association. p. 125-133. doi: 10.3384/ecp14096125

Lee LSH, Jim CY. 2019. Energy benefits of green-wall shading based on novel-accurate apportionment of short-wave radiation components. Appl Energy 238: 1506-1518. doi: 10.1016/j.apenergy.2019.01.161

Marino C, Nucara A, Pietrafesa M, Polimeni E. 2017. The effect of the short wave radiation and its reflected components on the mean radiant temperature: modelling and preliminary experimental results. J Build Eng 9: 42-51. doi: 10.1016/j.jobe.2016.11.008

Medl A, Stangl R, Florineth F. 2017. Vertical greening systems - A review on recent technologies and research advancement. Build Environ 125: 227-239. doi: 10.1016/j.buildenv.2017.08.054

Morakinyo TE, Lai A, Lau KKL, Ng E. 2019. Thermal benefits of vertical greening in a high-density city: Case study of Hong Kong. Urban For Urban Green 37: 42-55. doi: 10.1016/j.ufug.2017.11.010

Nasir MHA, Hassan AS. 2020. Thermal performance of double brick wall construction on the building envelope of high-rise hotel in Malaysia. J Build Eng 31: 101389. doi: 10.1016/j.jobe.2020.101389

Ng E, Chen L, Wang Y, Yuan C. 2012. A study on the cooling effects of greening in a high-density city: An experience from Hong Kong. Build Environ 47: 256-271. doi: 10.1016/j.buildenv.2011.07.014

Oliveira ELD, Salles MT. 2020. Relations between urban subsoil and climate change in different neighborhoods of Rio de Janeiro. Ambient Soc 23: e01782. doi:

10.1590/1809-4422asoc20190178r2vu2020l6td

Pan L, Chu LM. 2016. Energy saving potential and life cycle environmental impacts of a vertical greenery system in Hong Kong: A case study. Build Environ 96: 293-300. doi: 10.1016/j.buildenv.2015.06.033

Paudyal K, Baral H, Bhandari SP, Bhandari A, Keenan RJ. 2019. Spatial assessment of the impact of land use and land cover change on supply of ecosystem services in Phewa watershed, Nepal. Ecosyst Serv 36: 100895. doi: 10.1016/j.ecoser.2019.100895

Peng J, Dan Y, Qiao R, Liu Y, Dong J, Wu J. 2021. How to quantify the cooling effect of urban parks? Linking maximum and accumulation perspectives. Remote Sens Environ 252: 112135. doi: 10.1016/j.rse.2020.112135

Pianella A, Aye L, Chen Z, Williams NSG. 2017. Substrate depth, vegetation and irrigation affect green roof thermal performance in a mediterranean type climate. Sustainability 9(8): 1451. doi: 10.3390/su9081451

Price A, Jones EC, Jefferson F. 2015. Vertical greenery systems as a strategy in urban heat island mitigation. Water Air Soil Pollut 226: 247. doi: 10.1007/s11270-015-2464-9

The Paper. 2021. Enhancing cultural and climate leadership is key to sustainable development in the world's cities (1). https://www.thepaper.cn/newsDetail_forward_15637710.

Saiz S, Kennedy C, Bass B, Pressnail K. 2006. Comparative life cycle assessment of standard and green roofs. Environ Sci Technol 40(13): 4312-4316. doi: 10.1021/es0517522

Shafiee E, Faizi M, Yazdanfar SA, Khanmohammadi MA. 2020. Assessment of the effect of living wall systems on the improvement of the urban heat island phenomenon. Build Environ 181: 106923. doi: 10.1016/j.buildenv.2020.106923

Shahmohamadi P, Che-Ani AI, Etessam I, Maulud KNA, Tawil NM. 2011. Healthy environment: The need to mitigate urban heat island effects on human health. Procedia Eng 20: 61-70. doi: 10.1016/j.proeng.2011.11.139

Su M, Jie P, Li P, Yang F, Huang Z, Shi X. 2024. A review on the mechanisms behind thermal effect of building Vertical Greenery Systems (VGS): Methodology, performance and impact factors. Energy Build 303: 113785. doi: 10.1016/j.enbuild.2023.113785

Tan CL, Wong NH, Jusuf SK. 2014. Effects of vertical greenery on mean radiant temperature in the tropical urban environment. Landsc Urban Plan 127: 52-64. doi: 10.1016/j.landurbplan.2014.04.005

Wong NH, Tan AYK, Chen Y, Sekar K, Tan PY, Chan D, Chiang K, Wong NC. 2010. Thermal evaluation of vertical greenery systems for building walls. Build Environ 45(3): 663-672. doi: 10.1016/j.buildenv.2009.08.005

Yang Y, Gatto E, Gao Z, Buccolieri R, Morakinyo TE, Lan H. 2019. The "plant evaluation model" for the assessment of the impact of vegetation on outdoor microclimate in the urban environment. Build Environ 159: 106151. doi: 10.1016/j.buildenv.2019.05.029

Yang Y, Guo X, Liu G, Liu W, Xue J, Ming B, Xie R, Wang K, Hou P, Li S. 2021. Solar radiation effects on dry matter accumulations and transfer in maize. Front Plant Sci 12: 727134. doi: 10.3389/fpls.2021.727134

Zhang L, Deng Z, Liang L, Zhang Y, Meng Q, Wang J, Santamouris M. 2019. Thermal behavior of a vertical green facade and its impact on the indoor and outdoor thermal environment. Energy Build 204: 109502. doi: 10.1016/j.enbuild.2019.109502

Zhang Y, Guo X, Liao S, Wu D, Lv P, Wei Q. 2022. Multi-scale structure synergistic strategy: A transpiration inspired hierarchical aerogel evaporator for highly efficient solar-driven clean water production. J Environ Chem Eng 10(3): 107934. doi: 10.1016/j.jece.2022.107934

Zhao C, Zhang L, Yang Y, Zhang Y, Liu M, Yan J, Zhao L. 2022. Long-wave infrared radiation properties of vertical green façades in subtropical regions. Build Environ 223: 109518. doi: 10.1016/j.buildenv.2022.109518